SPE-194264-MS

Downhole Leak Detection: Introducing A New Wireline Array Noise Tool

Qinshan Yang, Jinsong Zhao, and Marvin Rourke, GOWell international, LLC

This paper was prepared for presentation at the SPE/ICoTA Well Intervention Conference and Exhibition held in The Woodlands, TX, USA, 26-27 March 2019.

Abstract

This paper will introduce a new generation wireline Array Noise Tool (ANT). This tool is used to detect downhole acoustic / vibration activities originating from fluid-structure friction flow. One of main applications in Well Integrity (WI) and Plug & Abandonment (P&A) for ANT is to locate leak sources in well completions and tubulars. The innovative sensor matrix and system configuration together with three novel data processing methods are studied and developed to address the following primary challenges;

1. Tiny acoustic leakage signals (-30dB to -60dB), for example, the minor leaks behind pipes or even inside the formation matrix,
2. Strong road-noise acoustic signal contamination from tool motion while dynamic logging,
3. Nonstationary and/or nonlinear signal distortions because of tool flexural vibrations, and
4. Downhole seismic noise.

The tool can be operated both in stationary logging and in dynamic logging.

The wide-band sensor matrix is designed with a unique configurable technique to form different measurement arrays. As a result, the tool can simultaneously acquire absolute and differential acoustic signals. By using this sensor matrix we are able to improve Signal-to-Noise Ratio (SNR) by up to 20 to 30dB. From the acquired data, we employ a multi-dimensional machine learning (ML) classification module, cascaded with cluster iteration to separate real leak signatures from other unwanted noise signals. After a data conditioning process, the wave velocity-domain decomposition method is utilized to further distinguish the leak signal propagation characteristics against other noise propagations to enhance overall SNR for leak detectability. Lastly we use a Bayesian likelihood analysis to identify the leak depth locations with a confidence index based on the information contained in both signal energy and signal velocity. We are able to achieve 15dB to 20dB SNR improvement from this data processing methodology. The system design goal is to eliminate unwanted acoustic noise that is not associated with leaks, while maintaining sufficient sensitivity to pick up minor leaks.

The tool has been logged commercially in the US, Middle East, East Asia, and Latin America. The tool performance has been validated through simulation, lab tests, and field logs. Field logging examples are demonstrating a leak detection success rate above 95%. Field cases include multi-annulus, low flow rate, and gas well field examples. Field results will be presented in this paper.

ANT instrument technology and the associated advanced processing methods are a new solution for detecting the leak source locations and monitor leak paths, especially, in Well Integrity (WI), Plug and Abandonment (P&A), and many other well applications.

Introduction

Downhole passive acoustic measurements or more simply "noise logs" have been in common use for over 40 years (Enright 1955, McKinley et al 1972). The logs have been used to locate downhole sources of acoustic energy principally originating from various fluid flow mechanisms. The early versions of these noise tools employed hydrophones which were submergible microphones lowered in to problematic wells and an operator literally listened via headsets for high amplitude noises. The most important application was listening for fluid leaks; i.e. sources of noise where none were expected. The 1970's saw the introduction of analog electronic tools which were designed to detect sound within the audible part of the acoustic spectrum. These tools typically measured via several band-pass filters between 1 kHz and 10 kHz, resulting in 3 or 4 amplitude curves displayed on the log (McKinley et al. 1972).

Modern digital noise tools have broadened the measurement range covering the audible through the ultrasound frequencies. By employing Fast Fourier analysis (FFT) the log output has evolved into a frequency vs energy map with excellent frequency and amplitude resolution.

Downhole acoustic signals are produced by fluid movements. Measurements taken over a wide frequency range enables effective behind pipe diagnostics of:

- Fluid movement through media such as well completion hardware and porous formations that generally produce noise
- Multi-phase bubble behavior such as expanding gas bubbles during production
- The fluid noise caused by friction in high velocity turbulent flow
- Noise frequency that is broadly dependent on orifice size through which fluid is flowing
- Noise intensity which generally increases with higher flow rate as well fluid type and pressure differential.

Spectral noise logging when coupled with other measurements such as high-resolution temperature logging has the following applications:

- Leak Detection
- Identification of production and injection zones
- Location of flow behind pipe
- Location of top of cement
- Flow rate profiling when used with thermal simulation and temperature inversion

Noise logging has traditionally been acquired station-by-station where the logging tool is held stationary to avoid "road-noise", which is unwanted noise caused by the tool moving during acquisition. Noise logging with stationary measurements has multiple drawbacks:

- Depth spacing between stations — often chosen between 1 to 100meters
- Long acquisition times with closely spaced stations (1-5 meters)
- Poor vertical resolution with far spaced stations (5-100 meters)

- Temperature and other logs acquired separately with a continuous logging pass

To overcome these limitations a new logging tool has been developed which allows continuous logging while reducing the unwanted road-noise and improving SNR with respect to flow related noise signals.

Sensor array design

The new noise logging tool has both differential and azimuthal sensors, resulting in optimized tool length without sacrificing low signal detection. Fig. 1 is a schematic of the array noise tool sonde. There are five levels in the sensor matrix. The spacing between each level is six inches. The upper and lower level has two azimuthal array elements. Each azimuthal element consists of four independent sensors oriented 90 degrees apart. The azimuthal sensors allow measurement of azimuthal, common-mode, and differential signals. The three center levels are configured to make differential measurements. Each differential level has two independent channels oriented at 90 degrees which are referenced as the X and Y channels. Overall the tool has eight azimuthal and six differential channels for a total of 14 array measurements.

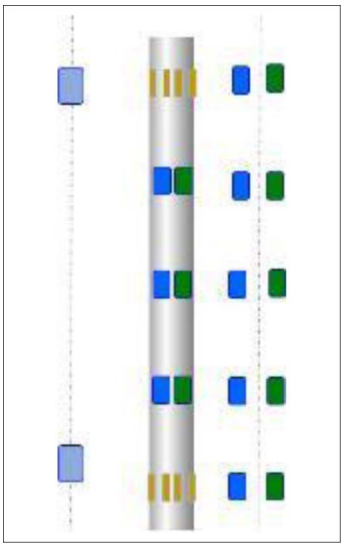

Figure 1—The array noise tool sonde schematic.

The four-channel azimuthal measurements at the upper and lower levels are processed in three ways;

1. Digital subtraction in X and Y orientation to output differential measurements. These are used with the center differential levels to form a five-element differential array.
2. summation of the four channels to output a common-mode signal for road noise evaluation and stationary measurements when required.
3. As individual azimuthal channels for a four-segment radial CBL measurement when tool is combined with an optional transmitter module.

Typical noise tool uses a monopole sensor which is highly sensitive to the road noise. One of the key concepts developed with the array noise tool is the use of differential signals which allow for cancelation of the common mode signals originating from the unwanted road noise generated while logging (Zhao and Yang, 2015). Fig. 2 illustrates the concept. Our field test results have confirmed that differential channels have up to 30 dB lower unwanted road noise signal levels compared with the common-mode or non-differential channel. Fig. 3 shows some field data comparing the noise levels between the differential channels and common mode (monopole) channels. The data was recorded during the same logging pass.

There is significantly less road noise in the differential measurements. Typical noise tool uses a monopole sensor which is highly sensitive to the road noise.

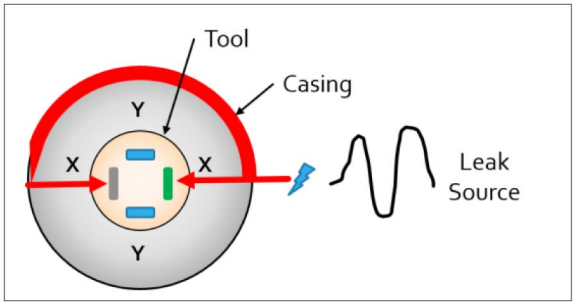

Figure 2—Why use differential measurements?

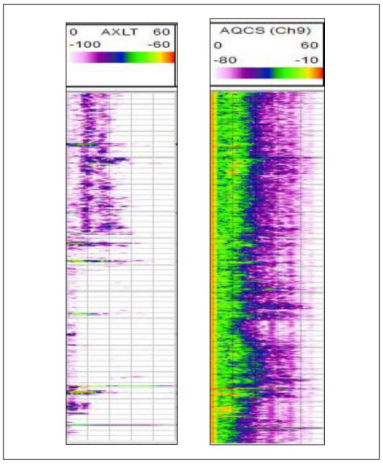

Figure 3—Differential measurements (left) compared to the monopole measurements (right).

Processing Algorithms

Array noise tool processing system inputs the down-hole measurements and transfers them into customers answer products. The processing includes both real-time on-site processing to give answers while logging and enhanced post-processing for thorough analysis. Real-time results are outputs that the field operator can quality-control data acquisition and highlight intervals where the causes of sound generation are likely. Final deliverables are based on the post-processing that combines some advanced processing algorithms, including wave velocity-domain analysis, Bayesian likelihood analysis, and machine-learning classification (Yang and Zhao, 2016).

While logging a passive noise tool records signal from a range of sources where the signal can be denoted as Eq. 1

$$\boldsymbol{S}(t) + n(t) \propto F_{Leak} + F_{Well}\left(f_{road} + f_{bump}\right) + F_{sys} + \sigma(S), \tag{1}$$

where, $S + n(t)$ is the measurement signal from one sensor; $F_{\text{Well}}(f_{Wroad} + f_{Wbump})$ is an environment related unwanted signal. f_{Wroad} is the road noise. f_{Wbump} is the 'bump' related high energy noise. These are the function of well geometries, fluid type, logging speed, logging direction, centralizer etc; F_{Leak} is wanted leakage signal. It is a function of well profile, geometries, fluid type, delta-Pressure, fluid rate, etc; F_{Well}, F_{Leak} and $\sigma(S)$ are all non-stationary random noise;

Typical signal-to-noise (SNR) ratio is below zero, in other word, the interference signal energy is higher than the leak noise signal. In general noise logging challenge is how to distinguish a weak leak signal from unwanted interference that have higher energy.

Wave velocity-domain

As a passive acoustic measurements tool, the array noise tool records the entire acoustic in-situ signal around the borehole. Eq. 1 describes the potential sources of the acoustic signals. There are three main types of acoustic signals the leak noise, road noise, and background noise. Those signals are contaminated with each other in both time and frequency domain. A range of finite difference method simulations were made to demonstrate the behavior of the passive acoustic measurements in the borehole. Fig. 4a shows the setup for the simulation.

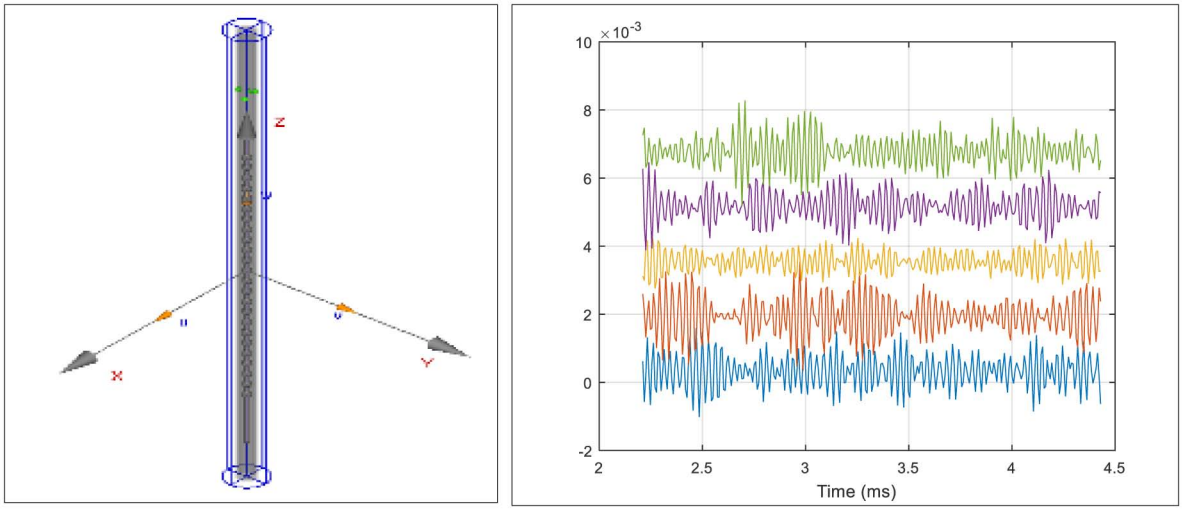

Figure 4—a) downhole acoustic passive measurement simulation; b) simulation measurements by differential channels

In the simulation, a borehole was setup with casing and cementing. There is a noise tool located in the center of the well. A four arms centralizer generates road noise and is simulated as four asymmetrical touch points on the casing shown as green dots in the Fig. 4a. Leak point is located on the casing and denoted as red dot in the Fig. 4a. Table 1 lists the related simulation parameters used;

Table 1—Simulation parameters

Name	Vp (m/s)	Vs (m/s)	Density (g/cm3)	Size (in)
Formation	4000	2300	2.5	---
Cement	2823	1729	1.92	7.8
Casing	6098	3354	7.5	6.3
Borehole	1500	---	1.0	---
Toolbody	3000	---	4.0	1.7

Fig. 4b displays the simulated results in time domain. There are five traces that demonstrate recorded measurement from each element in the array. Fig. 5 illustrates the frequency composition of the three component signals as discussed in Eq. 1. The key point to highlight is that the signals overlapped with each other in the frequency domain, which means the signals cannot be discriminated in either the time or frequency domain. We proposal an algorithm to separate the signals in the wave velocity-domain.

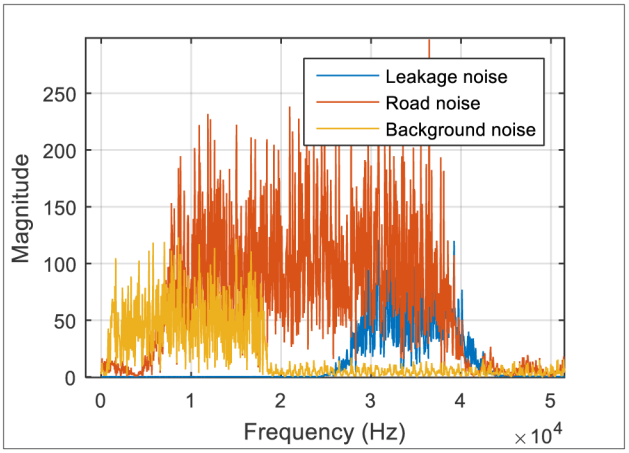

Figure 5—Simulation measurements in frequency domain;

Based on the facts that three groups signals cannot be differentiated from one another in either the time or frequency domain, we proposal an algorithm to separate signal in the wave velocity-domain. Fig. 6 shows the processing flow chart. The work space are all the input and output interface; work engine is the processing module; data library are pre-calculated data that prepared in advanced. One necessary processing module is the dispersion analysis. We extract frequency-slowness dispersion data from the group of acoustic waveforms. This is an extension Prony method that improve dispersion analysis by combing forward and backward methods (Ma, etc. 2010, Tang and Cheng, 2004). Assume that the observation data consists of P modes. In the frequency domain, the observed data is denoted as

$$\hat{X}_n(\omega) = \sum_{k=1}^{P} h_k z_k^{n-1} \qquad (n = 1,2,\cdots,N), \tag{2}$$

where $\hat{X}_n$ is the observed data in the frequency domain; N is the number of sensors in the array; h_k is the k_{th} mode in the signal; $z_k = \exp(-i\omega s_k d)$; s is the slowness and d is the distance between sensors. Prony and extended Prony method is commonly adopted to calculate slowness dispersion data from array sonic waveforms. Fig. 7a illustrates one dispersion analysis result from simulated leak passive acoustic array signal. Dispersion can also be done by Matrix-pencil (Sarkar and Pereira, 1995) method or the methods can estimate wave velocity at different frequency.

The propagation transform concept is based on the Radon transform (Deans, 2007). Radon transform is the integral transform integral of the function over a line with different slope. In our application, we define the propagation transform as

$$R(p,\tau) = \int_L g(\boldsymbol{M}) d\boldsymbol{M}, \tag{3}$$

where p is the slop of the integrated line, the propagation angle in this application. τ is its intercept. $g(\boldsymbol{M})$ is the dispersion curves. $\boldsymbol{M}$ is a function of frequency and wavenumber $2\pi fs$. s is the slowness of the wave propagation.

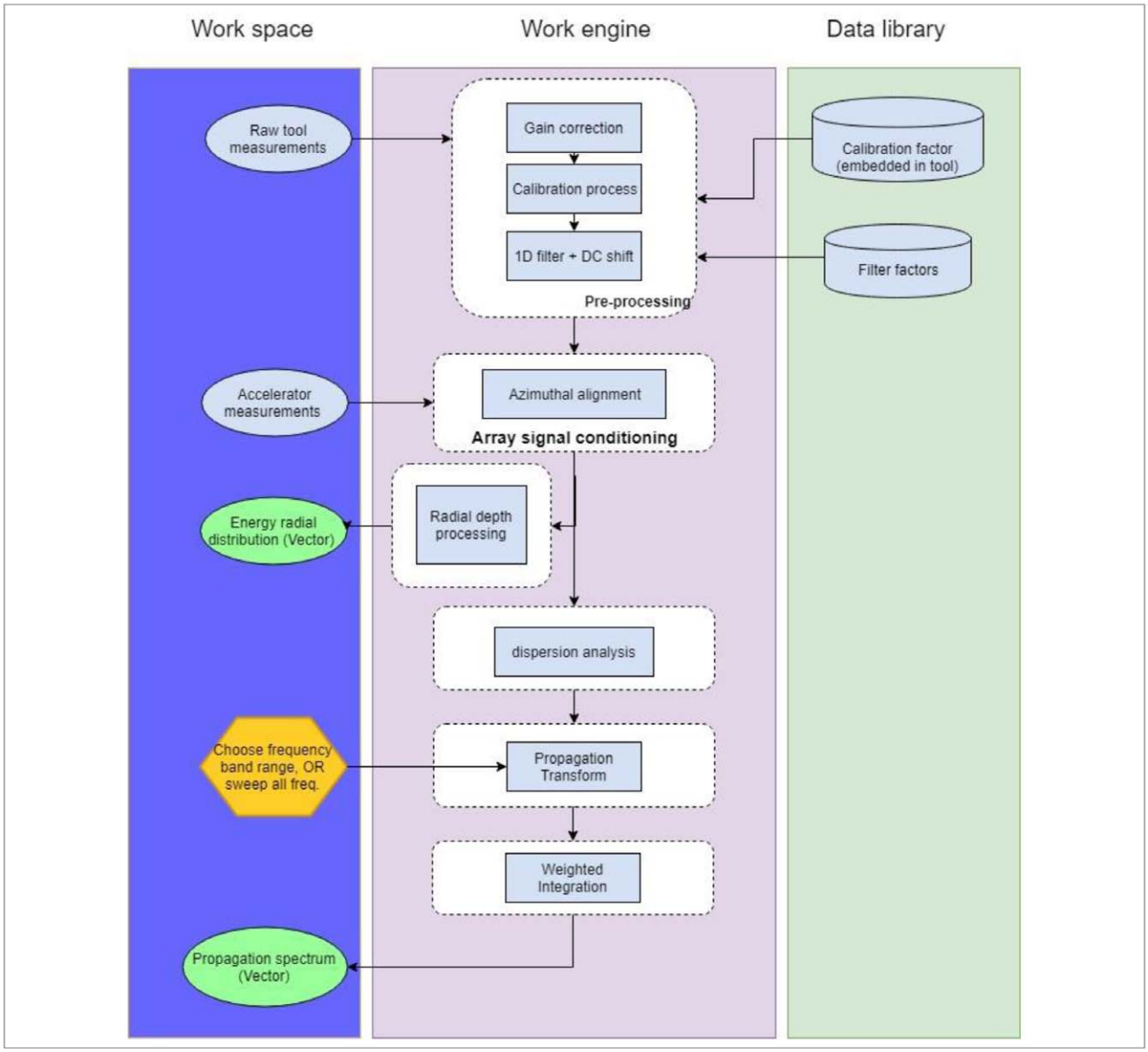

Figure 6—Processing algorithm flow chart

Fig. 7b demonstrates a propagation results based on the simulated array observed signal. In Fig. 7b X axis is the wave propagation angle, Y axis the intercept, Z axis is the propagation transform index. There is no unit for propagation transform index. The propagation degree that has higher index is the main propagation mode in the current acoustics array measurements;

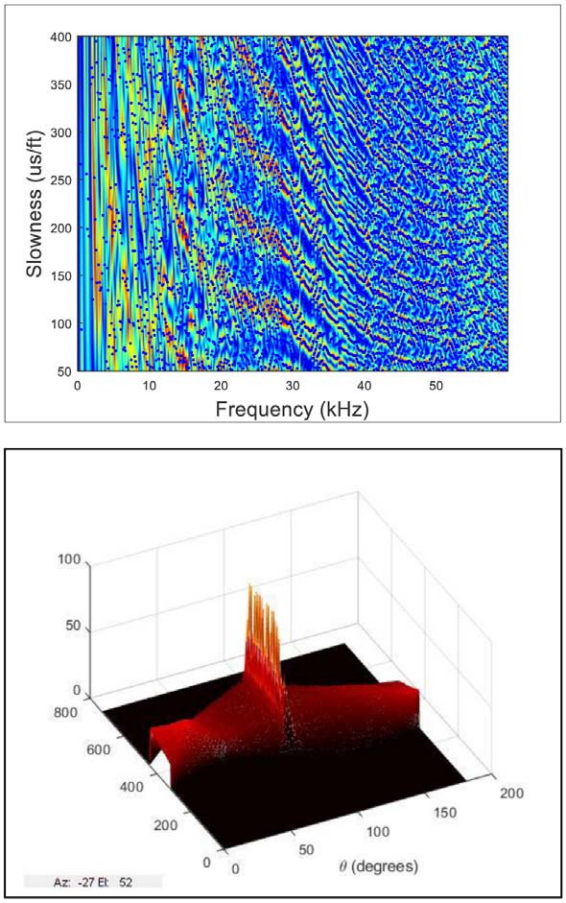

Figure 7—a) Dispersion analysis results; b) propagation transform processing

Bayesian likelihood analysis

Many factors will affect the passive noise acoustic signal in the downhole, include leaking condition, borehole profiling, fluid type, logging speed, etc. Given noise acoustic energy or leak point index only, one cannot tell there is a leak or not. We propose a probability analysis method to quantify the leak event probability. The relationship between leak event and the array noise tool measurement is referred to as the forward relationship, given by

$$\mathbf{G}(\boldsymbol{m}) = \boldsymbol{d}, \tag{4}$$

where **G** is the tool transform function, **m** is the leak event, **d = [Lpi, Am]** is the processing results based on observation data from the array noise tool. **Lpi** is the leap point index, **A*m*** is the amplitude. The leak detection performance is to estimate ***m*** from the available measurement. We denote the a-priori distribution of leak event as $p(\boldsymbol{m})$, the likelihood function as $p(\mathbf{d}|\boldsymbol{m})$, and the posterior probability for leak event as $q(\boldsymbol{m}|\boldsymbol{d})$.

We use Bayesian theorem to establish relationship between measurements probability and posterior probability. Bayes' theorem relates a priori and posterior distributions in a way that makes the computations of $q(\boldsymbol{m}|\boldsymbol{d})$ tractable (Aster et al., 2005). It can be written as

$$q(\mathbf{m}\,|\,\mathbf{d}) = \frac{p(\mathbf{d}\,|\,\mathbf{m})\,p(\mathbf{m})}{p(\mathbf{d})}, \tag{5}$$

$p(\boldsymbol{d})$ is a marginal likelihood and is not a function of model **m** . Thus, $p(\boldsymbol{d})$ will be absorbed as a constant, whereby Eq. 5 becomes

$$q(\mathbf{m}\,|\,\mathbf{d}) \propto p(\mathbf{d}\,|\,\mathbf{m})\,p(\mathbf{m})\,. \tag{6}$$

The prior distribution of parameters is determined from well condition knowledge or other external and independent information about leak. In general, the a priori model is a multidimensional probability distribution (Buland and Kolbjørnsen, 2012). It is assumed that properties in different layers are stochastically independent in the a-priori model. To minimize subjectivity in the leak detection, a discrete uniform distribution was imposed to obtain a-priori information. The probability mass function of the discrete uniform distribution is written as

$$p(C) = \begin{cases} \frac{1}{b-a+1}, & for\ a \le C \le b \\ 0, & C \le a\ or\ C \ge b \end{cases}, \tag{7}$$

where C_i denotes the unknown variable. For some leak detection measurements, we may know there is a leak in the well but try to figure out the position. In general, we set $a = 0$ and $b = 1$.

The likelihood function measures the probability of observing the data **d**, when the leak event is **m**. We denote the likelihood function as $p(\mathbf{d} \mid \mathbf{m})$. In our application, $\boldsymbol{d} = [\boldsymbol{Lpi}, \boldsymbol{Am}]$. Lpi is calculated in the wave velocity-domain. Amplitude is calculated in the spectrum domain. The likelihood function is defined by

$$\boldsymbol{p(d|m) = p(Am|m) \cdot p}\ . \tag{8}$$

To quantify the likelihood function (Yang and Torres-Verdín, 2014), we use a test well data as a reference calibration measurements. Amplitude information comes from waveform energy, there is no phase information involved. LPI information are calculated based on phase information, all waveform are normalized before processing. There is no energy information involved.

$$\begin{aligned} \boldsymbol{p(Am|m)} &\propto \frac{\boldsymbol{Am}}{\boldsymbol{Am_{ref}}} \cdot \boldsymbol{bh_{corrc}} \cdot \boldsymbol{fd_{corrc}} \\ \boldsymbol{p(Lpi|m)} &\propto \frac{\boldsymbol{Lpi}}{\boldsymbol{Lpi_{ref}}} \end{aligned} \tag{9}$$

By substituting the previous formula into Eq. 8, we can get the posterior distribution $q(\boldsymbol{m}|\boldsymbol{d})$ as apparent probability.

Classification from machine learning

During the continuously logging, the road noise is highly related with logging speed. Fig. 8 shows a field example that running with different logging speed. The road noise deeply affects the acoustic measurements and make the data unstable. Beside the wave-velocity domain signal processing, we propose a machine learning based clustering method to distinguish potential leak signal section, road noise section, and high energy bump section.

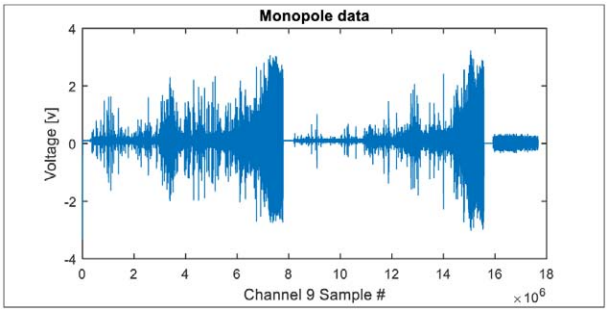

Figure 8—Passive acoustic signal value with different logging speed.

The data we used here comes from a noise tool logging job in South America. Fig. 9 demonstrates the raw spectrum results from the logging data. One can see many spiky bump signals in the spectrum data that make the noise detection vague.

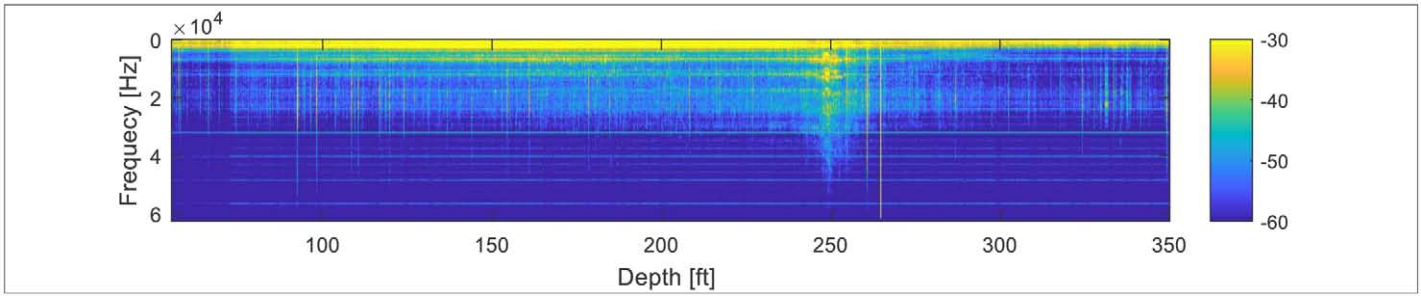

Figure 9—Passive acoustic signal spectrum at different depth.

We analyze two features of the signal to cluster the signal, the spectrum analysis and energy analysis. Spectrum analysis focus on the spectrum profiling after signal normalization. Fig. 10 exhibits spectrum profiling from different types of signal.

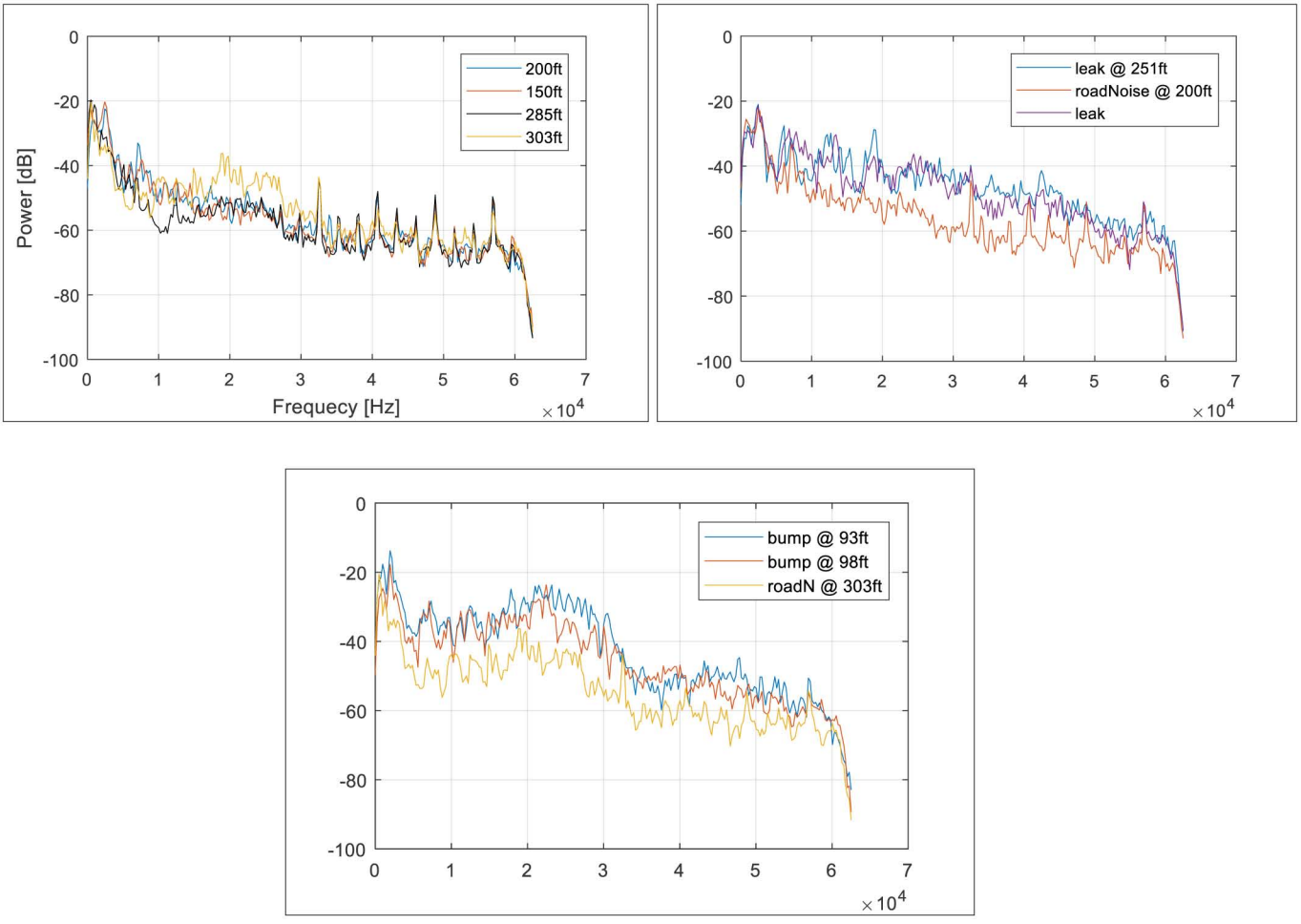

Figure 10—signal spectrum profiling from different signal group. From left to right, a) regular road noise; b) leak signal compare with road noise; c) high energy bump signal

We have these observations: road noise spectrum profiling is similar; leak noise spectrum profile is similar, and different with road noise; Most bump noise has similar road noise spectrum profile with different

amplitude. We use dynamic time warping (DTW) (Keogh, E. J. and Pazzani, M. J., 2001,) to quantify the similarity between spectrum profiling. Since all the signal are normalized before spectrum analysis, total energy of the waveform will not affect the spectrum analysis results.

Energy analysis is focus on the signal amplitude. Fig. 11 shows the signal energy different for different types of signals.

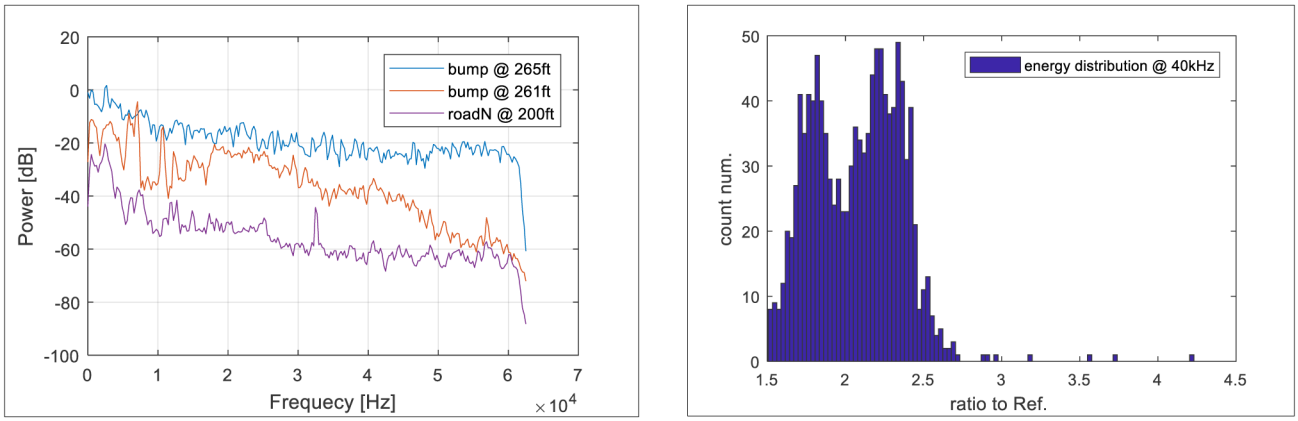

Figure 11—signal spectrum profiling from different signal group. From left to right, a) regular road noise; b) leak signal compare with road noise; c) high energy bump signal.

One can see the bump signal has relative high energy. On the energy distribution histogram, there are multi peaks that stands for different signal group with different energy. Consider the two features of signal, we will establish a two-dimensional features distribution. An unsupervised classification (Wagstaff, K., etc. 2001) is adopted to separate signal into four different groups. Fig. 12 shows the 2-D distribution base on the data measurements.

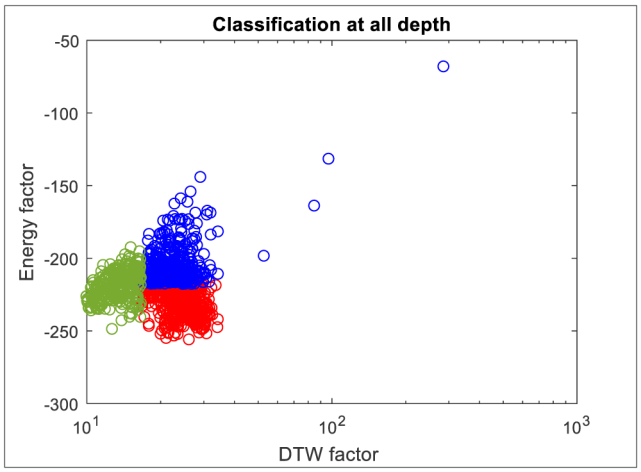

Figure 12—2-D distribution of signal grouping based on the DTW factor and energy factor.

Based on the signal group 2-D distribution, we will have four types of groups in the measurements.

- High energy road noise section: Similar spectrum curve with road noise;
- High energy bump section: high energy with different spectrum curve with road noise;
- Road noise section: similar spectrum curve with road noise;
- Potential leak signal section: low energy and different spectrum curves with road noise;

Fig. 13 displays the enhanced spectrum. After the clustering, we can reduce the road noise and bump signal's effect on the actual leak acoustic response that we want to observe. Real leak noise signal is observed clearly.

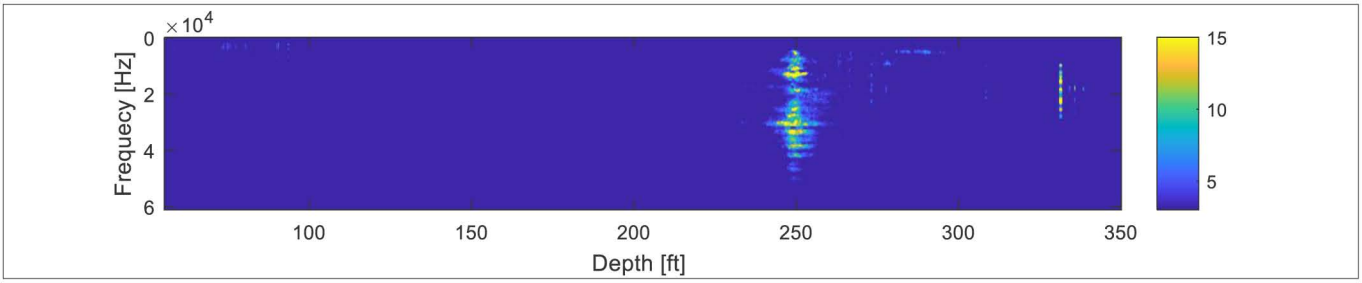

Figure 13—Passive acoustic signal spectrum at different depth after clustering processing

Tool Validation

Propagation analysis is one of the key features of the array noise tool that allows low SNR acoustic signals to be detected and utilized for source location. This section will provide validation results to confirm the propagation performance.

Fig. 14 shows the setup for the tool validation. The array noise tool is centralized in the pipe with outside diameter 3.5 in. A 500 psi pressure is built up in the pipe to make sure every validation has identical environment. In the bottom center of the pipe, there is a broadband hydrophone that can generate specific signal. In our validation, we use the hydrophone to generate background colored noise. A noise source continuously generates an acoustic signal to simulate sound of a leak source. We move the noise source along the pipe to simulate a logging operation in the borehole.

Figure 14—Array noise tool validation equipment.

Fig. 15a shows raw spectrum data. We can see the colored-noise across the whole logging interval. Leak noise source displayed from 20 to 200 second. There is no way to distinguish leak signal from the raw spectrum data with colored-noise. Fig. 15b illustrates the propagation analysis results on the raw data shown in Fig. 15a. We can see an ‘S’ pattern curve. During the down-logging, array noise tool is above the leak source at the start of logging. As the tool encounters the leak source, the acoustic wave propagation status will change from ‘up’ to ‘down’. This is the reason why we will see an ‘S’ pattern in the propagation analysis curve. The same occurs for the up-logging condition. The only different is that we will see a reversed ‘S’ pattern as shown Fig. 15d.

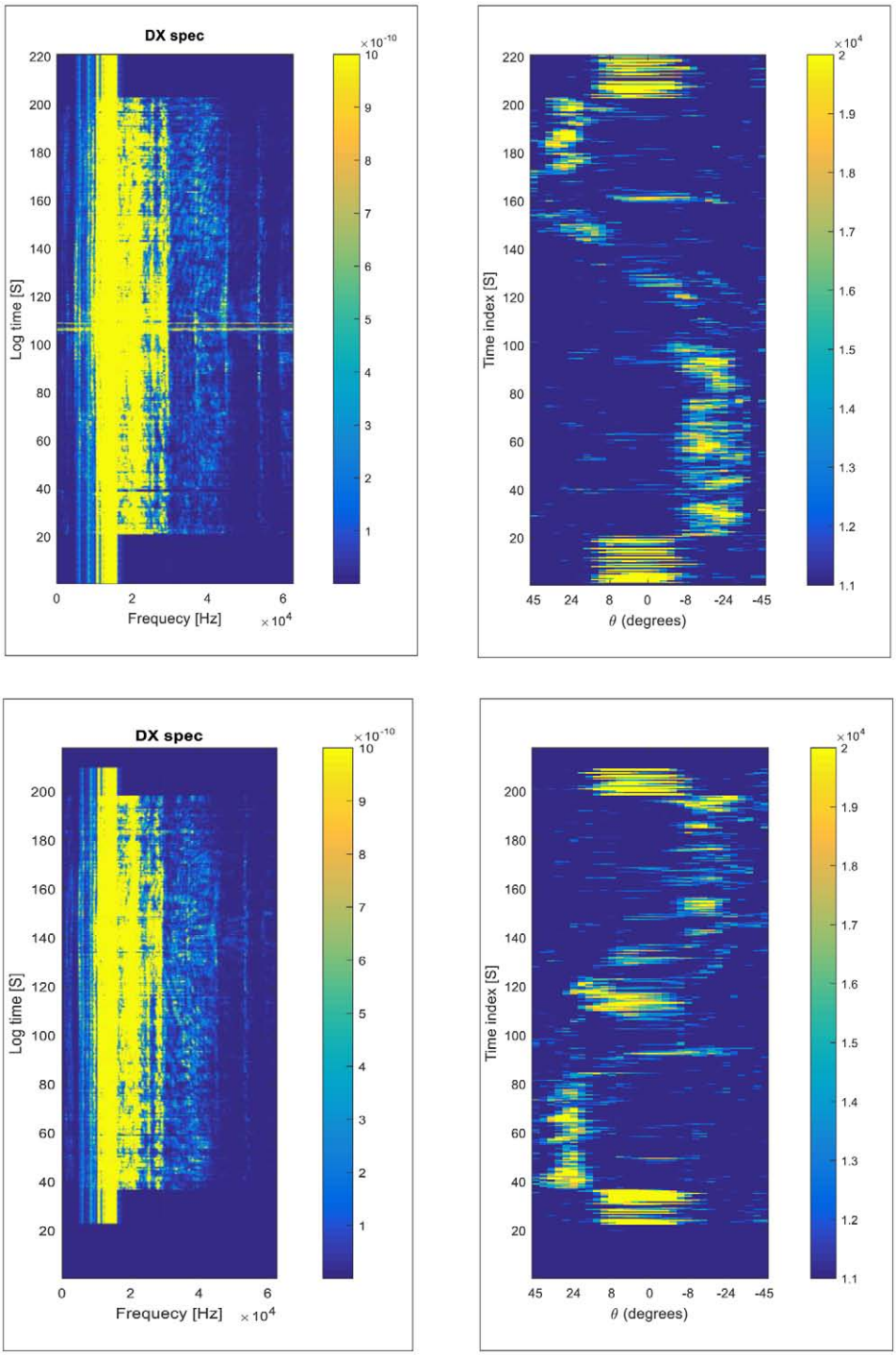

Figure 15—Validation raw data and processed propagation analysis results. From left to right: a) down-logging raw spectrum data; b) propagation analysis on down-logging data; c) up-logging raw spectrum data; d) propagation analysis on up-logging data;

Case Study Examples

Case 1 is a water injection well which developed a tubing to A-annulus communication while under injection. The logging procedure was for two runs, first run the well was under shut-in conditions and on the second run the well was on full injection with A-annulus open at the wellhead (BO-bleed off). The first run was the baseline log to record noise and temperature without an active leak while the second run was recorded under active leak conditions. A comparison between Shutin and BleedOff (BO) conditions is

shown in Fig. 16. As the well was under water injection the BO temperature is quite flat as it is dominated by the cooler injection water. It appears insensitive to the leak, whereas the noise data clearly shows high noise activity centered at a leaking tubing collar. From left to right the log tracks show:

- Depth
- BleedOff and Shutin Temperatures plus a CCL log acquired on the bleedoff pass.
- Raw noise log showing the differential frequency spectrum (0 to 60kHz) for the bleedoff pass
- Frequency bands curves showing total energy in 5-15khz, 15-30kHz, 30-45kHz and 45-60kHz for the bleedoff pass
- Enhanced differential spectrum (0 to 60kHz) for the bleedoff pass
- Propagation analysis (ADP) in two frequency bands (color map) and Leak Point Indicator (LPI) curve
- Enhanced differential spectrum from shutin pass
- Propagation analysis (ADP) from shutin pass

This example demonstrates how the advanced processing techniques are applied to field cases. The advanced processing (ADP) does not rely on noise amplitude but instead uses pattern recognition within the propagation analysis methodology. In this case the high amplitude noise as seen in the spectral analysis confirms the sensitive ADP results.

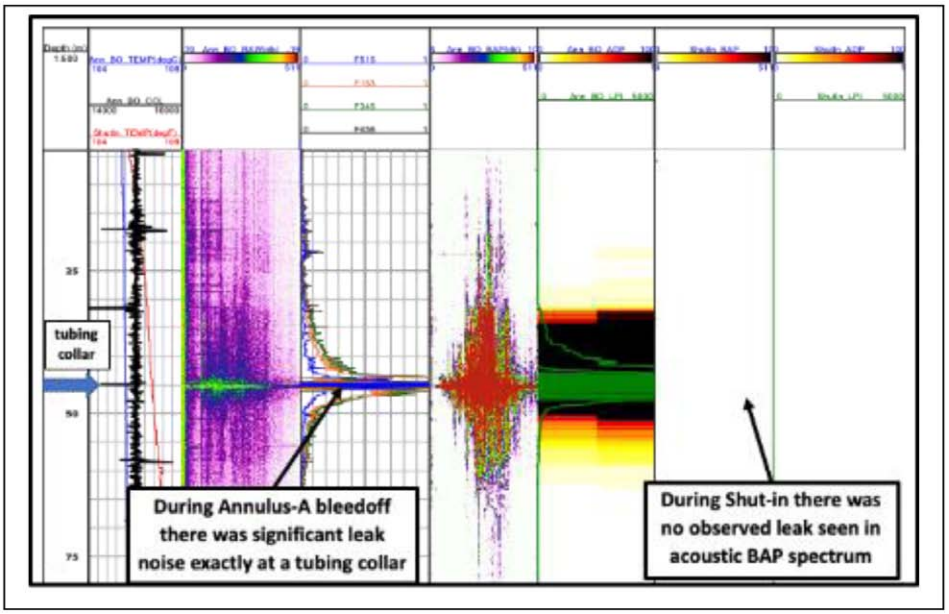

Figure 16—Example of tubing leak during water injection

Case 2 is a new gas production well which was experiencing A-annulus sustained pressure (SAP) problem. The logging program included running multi-finger caliper (MFC), EM thickness tool (MTD) and array noise tool (ANT). To activate and allow observation of the leak the annulus-A was allowed to bleedoff while logging. The well was shut-in, and a flare-line was connected to the A-annulus to allow the small amount of gas to be safely flared while logging. Fig. 17 shows a composite plot of all the data acquired with the array noise tool data in the rightmost four tracks and the pipe inspection logs in the leftmost tracks. The pipe inspection logs clearly show the location of the Tubing-Retrievable Safety Valve (TRSV) in the

7" tubing. From the array noise data, the leak point was found close to the center of the TRSV at the control line connection.

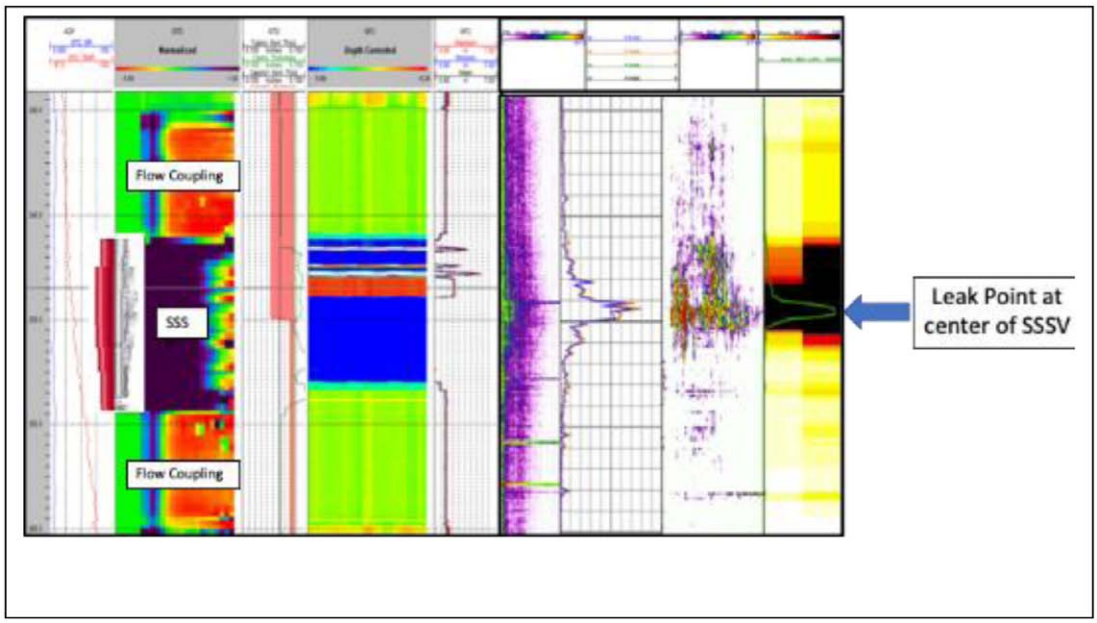

Figure 17—Example of noise log, multi-finger caliper and EM thickness data showing a leaking SSSV

Conclusions

We have developed and successfully verified a new array noise tool. This tool is designed to detect downhole leak sources and monitor leak-flow path. In the case of continuous logging, this new array noise tool addresses the challenge of weak acoustic leak identification that is contaminated by strong road noise signals.

We designed a sensor matrix that allowed creation of a differential sensor array. Field data has confirmed that differential channels exhibit 20~30 dB lower unwanted road noise signal level compared with traditional non-differential channels.

To process the non-stationary acoustic measurements, we proposed three processing modules; velocity-domain decomposition, Bayesian likelihood analysis, and machine learning classification. We are able to achieve 15 dB to 20 dB SNR improvement employing these data processing methods. Utilizing these processes, leak detection in the presence of high road noise, through multiple concentric pipe string, and very low-amplitude source signals is viable.

The array noise tool was verified in the lab, in field tests and commercial jobs in multiple regions world-wide. Field cases have included through multi-annulus leak cases, low flow rate leakage cases, and gas production well field examples, with a leak detection success rate of over 95%.

References

Aster, R. C., Borchers, B., and Thurber, C. H., 2005, Parameter Estimation and Inverse Problems: Elsevier Academic.

Buland, A. and Kolbjørnsen, O., 2012, Bayesian inversion of CSEM and magnetotelluric data. Geophysics, **77**(1), pp.E33-E42.

Deans, S.R., 2007, The Radon transform and some of its applications. Courier Corporation.

Enright, R.J. 1955, Sleuth for Down-Hole Leaks, Oil & Gas Journal.

Keogh, E.J. and Pazzani, M.J., 2001, April. Derivative dynamic time warping. In Proceedings of the 2001 SIAM International Conference on Data Mining (pp. 1-11). *Society for Industrial and Applied Mathematics*.

McKinley, R.M., Bower, F.M., and Rumble, R.C. 1972, The Structure and Interpretation of Noise Flow Behind Cemented Casing. Paper SPE 3999 presented at the SPE-AIME 47th Annual Fall Meeting, San Antonio, Texas, 8 — 11 October 1972.

Ma, J., Matuszyk, P. J., Mallan, R. K. et al., 2010, Joint Processing of Forward and Backward Extended Prony and Weighted Spectral Semblance Methods for Robust Extraction of Velocity Dispersion Data, SPWLA 51st Annual Logging Symposium.

Sarkar, T.K. and Pereira, O., 1995, Using the matrix pencil method to estimate the parameters of a sum of complex exponentials. IEEE Antennas and Propagation Magazine, **37**(1), pp.48–55.

Tang, X. M. and Cheng, A., 2004, Quantitative Borehole Acoustic Methods, Elsevier Ltd Press, ISBN: 0-08-044051-7.

Wagstaff, K., Cardie, C., Rogers, S. et al, 2001, June. Constrained k-means clustering with background knowledge. Vol. **1**, pp. 577–584.

Yang, Q. and Torres-Verdín, C., 2014, Joint interpretation and uncertainty analysis of petrophysical properties in unconventional shale reservoirs. Interpretation, **3**(1), pp.SA33–SA49..

Yang Q. and Zhao. J., 2016, Apparatus and Method of Propagation and Spatial Location Analysis by Acoustic Array for Down-hole Applications, US Patent No. 20180112523A1.

Zhao. J. and Yang Q., 2015, Apparatus and Method for a Matrix Acoustic Array, US Patent No. 9982527B2.